

Measurement of spatial resolution of a double-sided AC-coupled microstrip detector

L. Hubbeling, M. Turala and P. Weilhammer

CERN, CH-1211 Geneva 23, Switzerland

R. Brenner, I. Hietanen, J. Lindgren and T. Tuuva

University of Helsinki, Finland

W. Dulinski, D. Husson, A. Lounis, M. Schaeffer and R. Turchetta

LEPSI (ULP-IN2P3), Strasbourg, France

J. Chauveau

LPNHE, Paris VI, France

B.S. Avset and L. Evensen

S.I., Oslo, Norway

Capacitively coupled Si strip detectors with readout on both the p-side and the n-side have been developed. A novel scheme to separate strips ohmically on the n-side by means of field depletion via a suitable potential applied to the readout strips has been successfully demonstrated. Results on the spatial resolution of these detectors for both sides measured in a high energy beam are presented. The spatial resolution of the n-side has been measured at different incident angles of the beam tracks with respect to a vertical plane through the n^- strips at 0° , 20° and 40° .

1. Introduction

Microstrip detectors with p strips on n-doped silicon are today currently used in high energy physics experiments, fixed target as well as collider. Recently many efforts have been put into the development of double-sided microstrip detectors [1]. One high energy experiment (ALEPH at LEP) is already using double-sided microstrip detectors [2].

The realization of double-sided microstrip detectors is complicated by a technological problem. Fixed positive charges are always present in the oxide at the interface Si-SiO₂ at the end of the fabrication process. They attract electrons and an accumulation layer is built up. On the n-side this leads to a very low interstrip resistance and position information is lost.

A way to obtain a sufficiently high interstrip resistance is to create p^+ strips in between neighbouring n^+ strips. This isolation scheme has been successfully tested [1,2].

Our design takes advantage of the MOS structure naturally available in an AC-coupled detector. The aluminium readout strips are made larger than the

underlying n^+ strips. Thus the part of the readout strips that extends beyond the n^+ strips can be used as field plates to control the interstrip resistance by field depletion. Test beam results on a prototype are presented in this paper.

The design of the detector is described in section 2. In section 3 the beam test setup is illustrated and in section 4 the criteria of the off-line analysis are presented. In section 5 results are presented.

2. Detector design

The design of the AC-coupled double-sided microstrip detector (DS detector) we have tested has been thoroughly described in a previous paper [3]. Here we summarize the main features (see fig. 1).

The starting material is n-type silicon, about 5 k Ω cm resistivity and 280 μ m thick. The chip size is 22.5 mm by 22.5 mm and has a 2 mm wide boundary for mounting. The active area is surrounded by a 300 μ m wide guard ring. On both sides capacitors are integrated on the detector to allow AC coupling to the

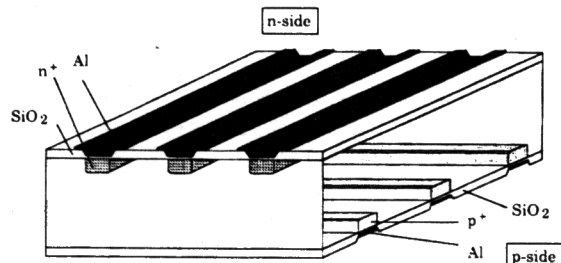


Fig. 1. Cross section 3D view of the double-sided detector.

readout electronics. Bias is provided through individual integrated polysilicon resistors between the strips and the bias bus line. On both sides there are 384 strips, 10 μm wide and with a pitch of 50 μm .

On the p-side the aluminium readout lines are 10 μm wide. On the n-side these lines are made larger than the underlying diffused strips to allow ohmic isolation of neighbouring strips via field depletion. The n-side has been divided into three regions, each of 128 strips. On each region a different width of the aluminium readout line has been chosen: 20, 30 and 40 μm . Observe that no extra masks or processing steps are required on the n-side in comparison with the p-side.

During the tests the strips on the p-side were grounded while the full depletion voltage (over 50 V) was applied to the n-side.

Since the working point for the electronics on both sides was of about 4.5 V, a negative field plate voltage of over 45 V is effectively applied.

Measurements indicate [3] that a sufficiently high interstrip resistance can be achieved with this method.

3. Beam test setup

The beam test setup is shown in fig. 2. The beam was a pion beam with momentum higher than 200 GeV/c so that multiple scattering was negligible.

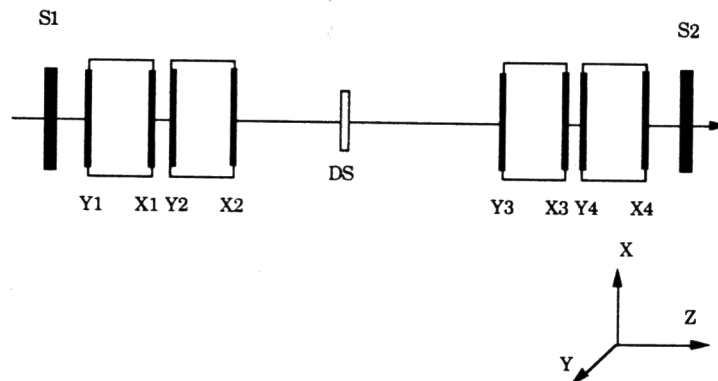


Fig. 2. Beam test setup.

Eight single-sided microstrip detectors provide a precise track reconstruction. They are of the same type as the ones used in the DELPHI microvertex detector [5]: AC-coupled with individually integrated polysilicon resistors for each diode. 25 μm pitch and 50 μm readout pitch, 640 strips each. These detectors were equipped for readout with NMOS microplex chips [6].

For the readout of the DS detector we used CMOS MX3 chips [7].

Five Sirocco CAMAC units [8] digitize the analog signals. The on-line acquisition program runs on a VME Eurocom 5 module [9].

Reference detectors are mounted in pairs. In each pair one detector measures the vertical coordinate (X) while the other measures the horizontal one (Y). The DS detector is mounted on a rotating stage, n-strips vertically (thus measuring Y) and p-strips horizontally. The rotation axis is vertical. The whole system, reference detectors plus DS, consists of about 6000 channels.

4. Off-line analysis

Raw data are processed off-line and pulse-height and noise for each channel are calculated after subtraction of the pedestal and of the commonmode shift (see [5] for a detailed description of the calculations).

Clusters are selected according to the following criteria. First we look for a strip with $(S/N)_{\text{strip}} > T_1$; then, all the neighbouring strips with $(S/N)_{\text{strip}} > T_2$ are included in the cluster. Eventually the cluster is accepted if: (i) $(S/N)_{\text{cluster}} > T_3$; (ii) $(S)_{\text{cluster}} > T_4$ ADC counts; (iii) the number of strips in the cluster is smaller or equal to T_5 .

All the thresholds, T_1 to T_5 are detector dependent. Table 1 shows the values of the threshold used for the DS. The value of 0 for T_2 (i.e. strips are accepted in the cluster if their signal is positive) was chosen in

Table 1
Lists of thresholds used in cluster analysis of DS detector

	T_1 cut on central strip	T_2 cut on neighbour strips	T_3 cut on cluster S/N	T_4 cut on cluster S	T_5 cut on # strip
P-side	3.0	0.0	8.0	20.0 ADC count	9
N-side	3.0	0.0	6.0	20.0 ADC count	9

order to have no bias in the analysis of the position resolution (see section 5).

Hit positions are calculated making a nonlinear interpolation on the signals of the two strips with the highest signals in the cluster.

Only tracks fully reconstructed in space by the reference detectors are used for the alignment. For the study of the resolution of the double-sided detector we select a window of $\pm 100 \mu\text{m}$ around the predicted impact point and we look for hits in this region.

5. Results of the DS detector

5.1 Data at 0°

Fig. 3 shows a plot of the pulse-height on the p-side vs the pulse-height on the n-side. As expected, the correlation is linear.

Projecting the plot on the two axes gives the Landau distributions for each side separately (fig. 4). The peak positions are, for both distributions, at about 37 ADC

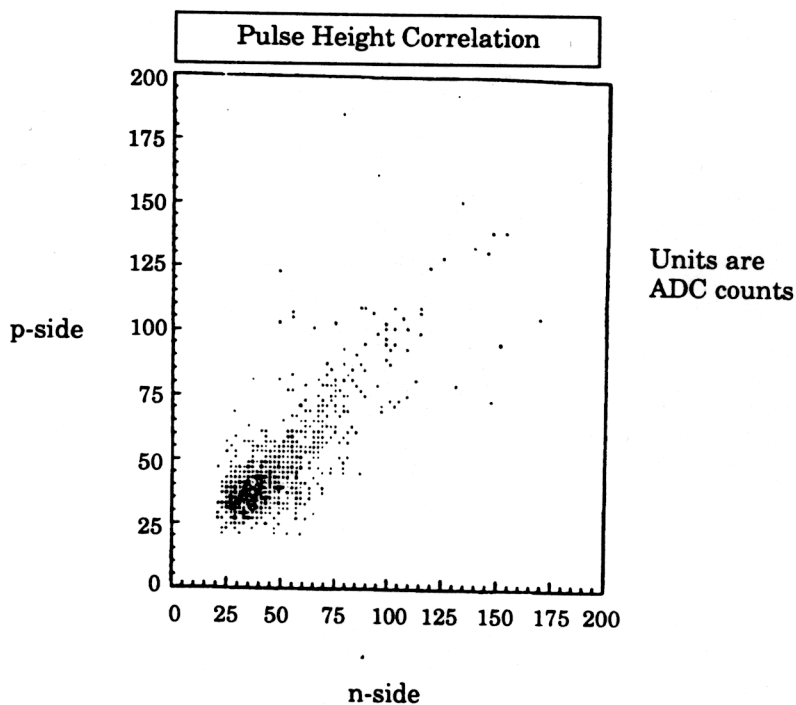


Fig. 3. Plot of pulse-height on p-side vs. pulse-height on n-side.

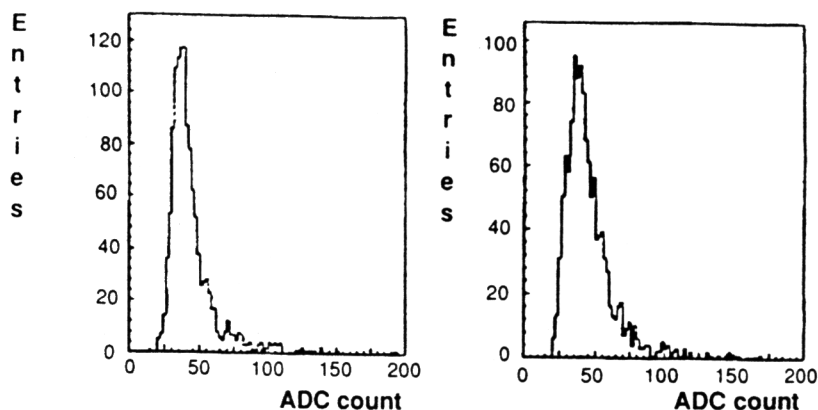


Fig. 4. Landau distributions for (a) p-side and (b) n-side.

counts. Given the average noise of 2.3 ADC counts for the p-side and of 3.6 ADC counts for the n-side, we can calculate a S/N of about 16 for the p-side and of about 10 for the n-side. The noise on the n-side is on average about 50% higher than on the p-side. This effect may be caused by a varying parasitic bias resistor of an accumulation layer channel under the polysilicon resistor. We are studying this effect at present.

On both sides the efficiency is higher than 98%.

In fig. 5 the residue distributions for each side are shown, together with a Gaussian fit. The sigmas of the fits are 9.6 and 12.4 μm , respectively for the p- and for the n-side. Given the errors on the reconstructed impact points of 3.9 and 4.5 μm , we can subtract these errors quadratically from the fitted sigma, obtaining a resolution of 8.8 and 11.6 μm respectively. The slightly

worse resolution of the n-side is fully compatible with the worse signal over noise ratio found on the n-side.

It is apparent that the Gaussian fits deviate from the experimental distributions. This fact is not due to the quality of data but to the intrinsic behaviour of the detector.

After a particle has traversed the detector, the electrons and holes created drift towards the collecting electrodes and at the same time diffuse. The width of the diffusion cloud is measured to be around 10 μm [10]. So when a particle traverses the detector close to a strip, charge is collected mainly by one strip. True charge sharing with a neighbouring strip will be completely masked by noise. A small fraction of the signal will appear at the input of the two neighbouring amplifiers due to the capacitive coupling. No correction for

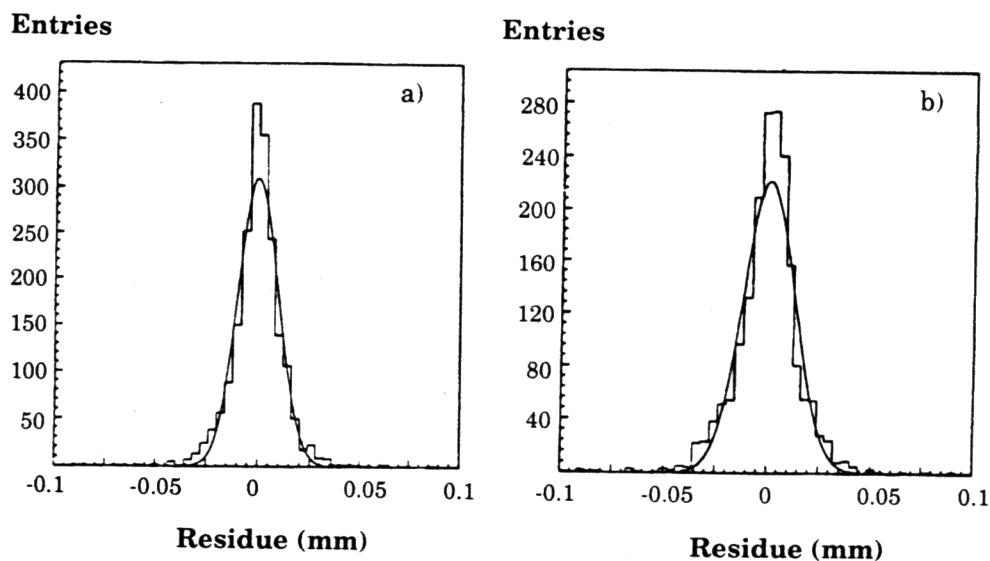


Fig. 5. Residuals distribution at 0° with 1-Gaussian fit. (a) p-side, (b) n-side.

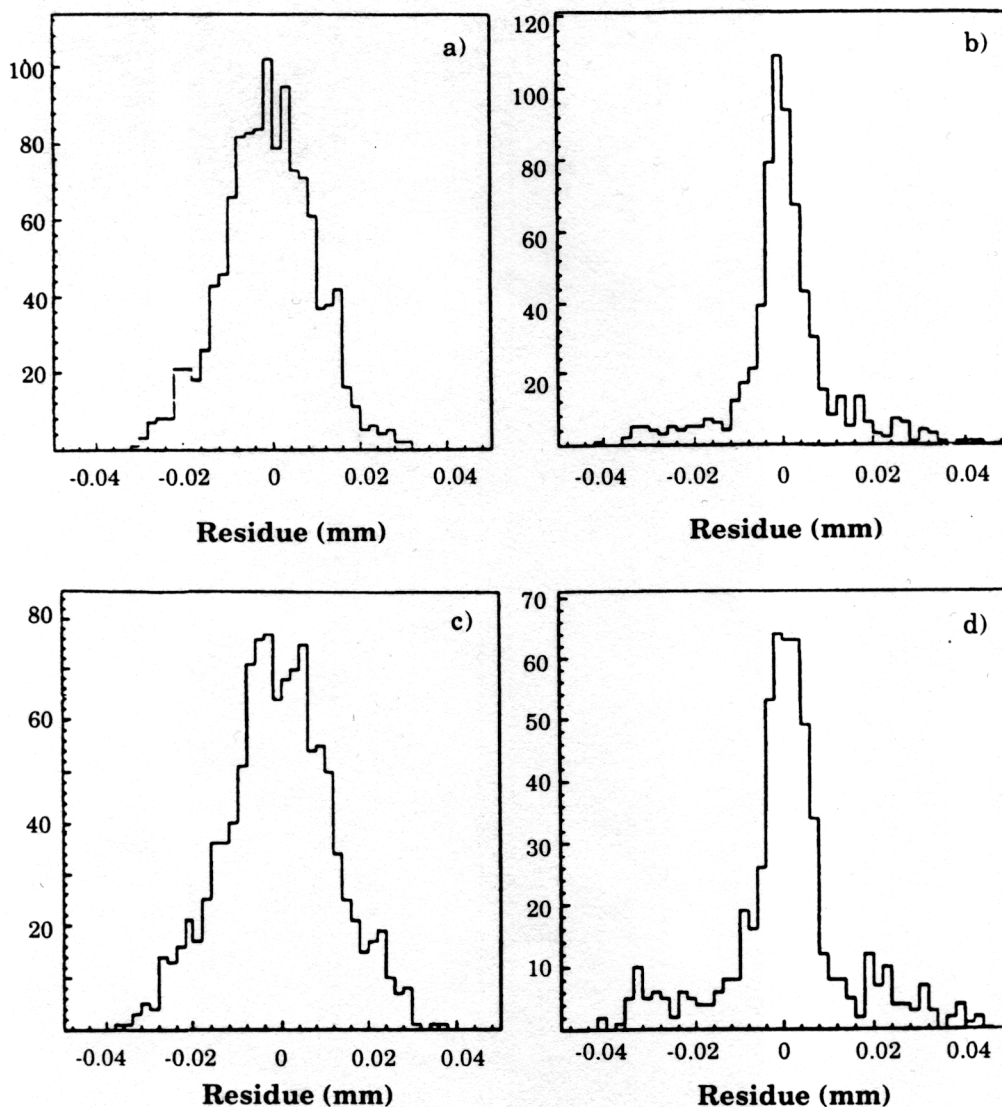


Fig. 6. Residuals distribution for the regions A and B (see text) for both sides. (a) p-side, region A: FWHM = 20 μm ; (b) p-side, region B: FWHM = 8 μm ; (c) n-side, region A: FWHM = 24 μm ; (d) n-side, region B: FWHM = 12 μm .

this effect is done in this analysis. When the particle crosses the detector in the middle region between two strips, the charge sharing on two strips due to the diffusion is effective.

In order to demonstrate this effect we have divided the detector volume into two regions: region A extending 15 μm sideways of a strip; region B including the 20 μm in the middle between two strips. Given an extrapolation error of about 4 μm , this selection should give rather significant separation of the two types of charge sharing. Residual distributions taken separately for the two regions are shown in fig. 6; for both the n-

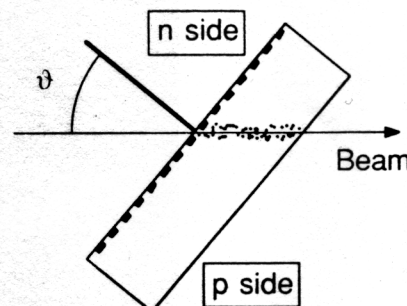


Fig. 7. Geometry of data taking with inclined tracks.

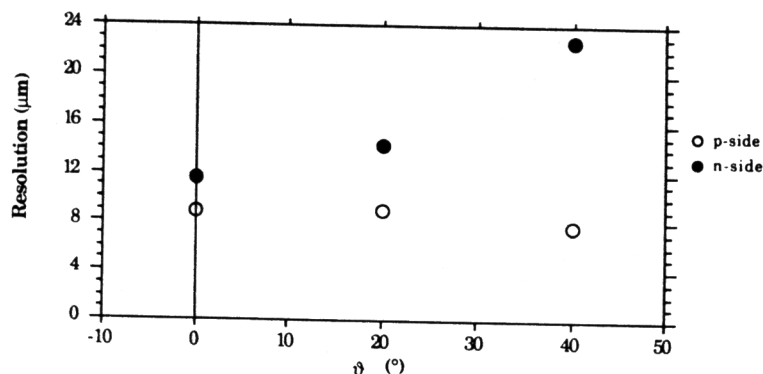


Fig. 8. Plot of resolution on p- and n-side as a function of the angle.

and the p-side, the FWHM of the region B is about half of that of region A.

5.2. Data taken with inclined tracks

As stated in section 1, we have also taken data with the detector inclined. The geometry is shown in fig. 7. Two geometrical effects contribute to modify the resolution of the detector with respect to the data taken at 0° .

(i) The path of particles in the silicon, and therefore the charge released in the silicon, is increased by a factor $1/\cos \vartheta$; (ii) the projection of the path along the coordinate measured on the n-side is increased by a factor $\tan \vartheta$, while it stays unchanged for the p-side. This second effect means that the signal is collected on several strips. What we expect from these two effects is a worsening of the resolution of the n-side for increasing angle, and possibly a slight improvement on the p-side due to better S/N ratio.

We have collected data with the detector inclined by 10° , 20° , 40° and 60° . In fig. 8 we show the measured resolution for two angles. For data taken at 20° and 40° , a *centre-of-gravity* algorithm was used to calculate the position of the hits on the n-side. Shown resolutions are obtained from the sigma of a Gaussian fit to the residual distribution to which the error on the impact point has been subtracted in quadrature. These results are preliminary and further analysis using a more refined algorithm is at present being performed, including the data taken at 10° and 60° .

6. Conclusions

We have tested an AC-coupled double-sided detector in a beam line with minimum ionizing particles. A novel isolation scheme for n^+ strips, based on field depletion, has been used. Although the design of the detector was not optimized for position resolution, we

achieved a spatial precision of $11.6 \mu\text{m}$ on the n-side and $8.8 \mu\text{m}$ on the p-side, consistent with the strip and readout pitch ($50 \mu\text{m}$) chosen and with the observed S/N values for both sides. Data have also been taken with inclined tracks and show that a resolution of at least $25 \mu\text{m}$ for the n-side is obtainable for tracks at 40° .

These results make us confident on the use of this detector in experiments. An improved version of this detector will be used in the upgrade of the DELPHI microvertex detector.

References

- [1] K. Saito et al., these Proceedings (2nd London Conf. on Position-Sensitive Detectors, London, UK, 1990) Nucl. Instr. and Meth. A310 (1991) 175; G. Batignani et al., ibidem, A310 (1991) 160.
- [2] H.-G. Moser, these Proceedings (2nd London Conf. on Position-Sensitive Detectors, London, UK, 1990) Nucl. Instr. and Meth. A310 (1991) 490.
- [3] B.S. Avset et al., IEEE Trans. Nucl. Sci. NS-37 (1990) 1153.
- [4] M. Berger and A. Both, PROUDS, Universität Duisburg-Gesamthochschule, July 1989.
- [5] V. Chabaud et al., Nucl. Instr. and Meth. A292 (1990) 75.
- [6] J.T. Walker et al., Nucl. Instr. and Meth. 226 (1984) 200.
- [7] P. Sella et al., IEEE Trans. Nucl. Sci. NS-35 (1988) 176.
- [8] SIROCCO, CERN EP electronics note 86-01.
- [9] Eurocom 5 is built by Eltec Elektronik GmbH; Galileo-Galileistr. 11, D6500 Mainz 42.
- [10] E. Belau et al., Nucl. Instr. and Meth. 214 (1983) 253.